

## Feasibility study to design a particle deposition unit utilizing electrophoresis for off-line measurements

Jung Hyeun Kim<sup>†</sup>

Department of Chemical Engineering, University of Seoul, 90 Jeonnong-dong Dongdaemun-gu, Seoul 130-743, Korea  
(Received 2 March 2007 • accepted 12 July 2007)

**Abstract**—Nanoparticles are widely used in various applications such as catalysts, mechanical polishing, composite materials, size standards, and structural templates. For those applications, sometimes it is necessary to sample nanoparticles onto clean substrates and onto a designated area. In this article, electrophoresis is demonstrated as a very feasible method to sample the desired number of particles onto a specific area of a substrate without contamination problems. In addition, an analytical equation was derived for estimation of deposition area, and compared with the experimental results. Pure copper particles generated by spray pyrolysis were used for size-classifications and depositions. Particle depositions were performed at 2,000 V and 7,000 V, and light scattering parameters from those deposited samples were measured; results showed good agreement of deposition area between estimations and measurements. Therefore, the use of the electrophoresis is promising in sampling particulates onto clean substrates without contamination and onto the designated sampling area with controlled number density.

Key words: Nanoparticles, Electric Field, Aerosol, Deposition

### INTRODUCTION

Nanoscale particulates have been widely used in various applications such as catalysts, mechanical polishing, composite materials, size standards, and structural template. Amongst various particle generation techniques, aerosol methods have a big advantage in preventing contamination, for example, compared to solution generation techniques [1-6]. Particle sampling is sometimes required on a very clean substrate, because, for example, light scattering metrology is quite sensitive to the presence of any contaminant materials [7,8]. Various sampling methods such as low pressure impactor, dipping into solution and drying, thermophoresis, and electrophoresis are possible to deposit particles on designated substrates. A low pressure impactor can focus particles onto a very narrow deposition area, but it can produce bouncing problems because of the high inertial force of high speed particles through the impactor nozzle. Therefore, it is very hard to control particle number density by using the low pressure impactor. Dipping technique would leave various residual matters on the target substrate after drying. Thermophoresis can be used for small particle sampling onto a substrate using temperature gradient, but it is not easy to control the deposition area because the surface temperature should be controlled for every different targeted area. Finally, the electrophoresis method [9,10] is quite useful in controlling deposition area with experimental parameters: particle diameter, particle flow rate, electric field force, separation distance between two electrodes.

In the application of electrophoresis for particle sampling, the biggest advantage is that the particle material is not a function of the electric field. Therefore, any particulate matters can be deposited with the same deposition condition for the same deposition area. Once a particle possesses a negative or positive charge, it can be

controlled by the experimental parameters under the electric field.

In this manuscript, designing procedures for constructing an electrostatic sampling unit for off-line measurements are described. For analytical estimation of the deposition area, deposition radius was obtained from the simple flow equation by applying boundary conditions. Parameters to control the deposition area are particle diameter, particle flow rate, separation distance, and electric field strength. Several example calculations were performed using those parameters. For experimental investigations, pure copper particles produced from spray pyrolysis method were used. Copper particles were size-classified through a differential electrical mobility analyzer for deposition onto silicon substrates. The deposited samples were tested by the optical light scattering instrument, and the light intensity scattered by the particles was recorded for analysis. Finally, the experi-

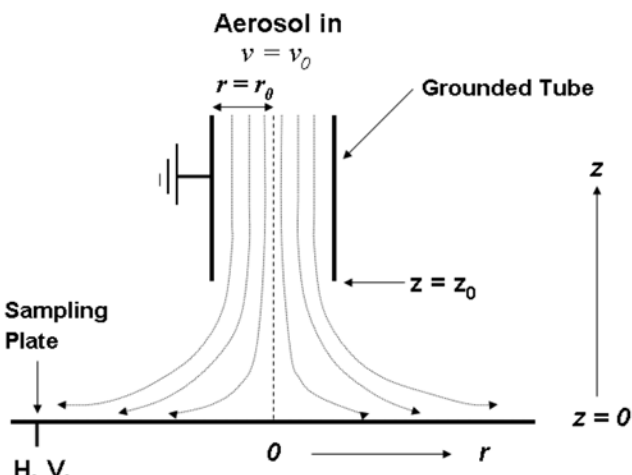


Fig. 1. Schematic drawing showing plane flow of the charged aerosol particles. Inlet tube is grounded and high voltage (H.V.) is applied to the sampling plate.

<sup>†</sup>To whom correspondence should be addressed.  
E-mail: jhkimad@uos.ac.kr

mentally measured deposition area was compared with the analytically estimated value.

## CALCULATION OF DEPOSITION AREA

In order to estimate deposition area, plane aerosol flow containing charged particles is considered as shown in Fig. 1. As the aerosol stream approaches to the plane  $z=0$ , the fluid turns to one side by the corner and departs in the  $r$  direction by plane flow.

$$v_1 = v_1(r, z) \quad (1)$$

$$v_2 = v_2(r, z) \quad (2)$$

$$v_3 = 0 \quad (3)$$

Velocity potential can be given by  $\Phi = \Phi(r, z)$  and it can be expanded by Taylor series expansion at the origin [11].

$$\begin{aligned} \Phi = \Phi(0, 0) + r \frac{\partial \Phi}{\partial r}(0, 0) + z \frac{\partial \Phi}{\partial z}(0, 0) + \frac{1}{2}(r)^2 \frac{\partial^2 \Phi}{\partial r^2}(0, 0) \\ + rz \frac{\partial^2 \Phi}{\partial r \partial z}(0, 0) + \frac{1}{2}(z)^2 \frac{\partial^2 \Phi}{\partial z^2} + \dots \end{aligned} \quad (4)$$

By applying boundary conditions

$$v_1 = -\frac{\partial \Phi}{\partial r} = 0 \quad \text{at} \quad r=0 \quad (5)$$

$$v_2 = -\frac{\partial \Phi}{\partial z} = 0 \quad \text{at} \quad z=0 \quad (6)$$

$$\therefore \frac{\partial \Phi}{\partial r}(0, 0) = \frac{\partial \Phi}{\partial z}(0, 0) \Rightarrow \frac{\partial^2 \Phi}{\partial r \partial z}(0, 0) = 0 \quad (7)$$

Thus, the Laplace equation must hold everywhere, in particular at origin.

$$\frac{\partial^2 \Phi}{\partial r^2} + \frac{\partial^2 \Phi}{\partial z^2} = 0 \Rightarrow \frac{\partial^2 \Phi}{\partial r^2} = -\frac{\partial^2 \Phi}{\partial z^2} = k \quad (\text{constant}) \quad (8)$$

Since the velocity profile is arbitrary to a constant, we can choose to define  $\Phi(0, 0) = 0$ . Then, the velocity potential can be defined as

$$\Phi = \frac{k}{2}(r^2 - z^2) \quad (9)$$

Then, corresponding velocity components are

$$v_1 = -\frac{\partial \Phi}{\partial r} = -kr \quad \text{and} \quad \frac{dr}{dt} = -kr \quad (10)$$

$$v_2 = -\frac{\partial \Phi}{\partial z} = kz \quad \text{and} \quad \frac{dz}{dt} = kz \quad (11)$$

In Eq. (11),  $v_2 = v_0$  at  $z=z_0$ , so  $k = -v_0/z_0$ .

From Eq. (10), the deposition radius can be expressed as  $r = r_0 \exp(-kt)$ .

In the presence of an electric field ( $E$ ) between the aerosol inlet and the deposition substrate, the charged particles will have an additional velocity component in the electric field direction for the amount of  $-v_E$ . Therefore, Eq. (11) becomes

$$\frac{dz}{dt} = kz - v_E \quad (12)$$

We are interested in computing the time ( $t_p$ ) at the distance of  $z=0$ . Simple integration of Eq. (12) gives the precipitation time under the electric field,  $E$ :

$$t_p = \frac{1}{k} \ln \left[ 1 - \frac{z_0 k}{v_E} \right], \quad (13)$$

so, the radius for the particle deposition can be

$$r_p = r_0 \exp(-kt_p). \quad (14)$$

From Eq. (14), it is seen that every radial position is related by the same factor based on the electric field force, so the exit concentration will be uniform if the inlet concentration is uniform. The velocity component ( $v_E$ ) in a certain electric field can be determined from particle mobility and applied field force:  $Z_p = v_E \cdot E$  [12].

## EXPERIMENTAL

### 1. Particle Generation

A spray pyrolysis system was used in this study, consisting of particle generation, classification, and collection units. Precursor solutions (0.30 mol/L) were prepared from copper nitrate  $[\text{Cu}(\text{NO}_3)_2 \cdot 2.5\text{H}_2\text{O}]$  precursor. The precursor was reagent grade and was used without further purification. A precursor solution was atomized with a Retec type nebulizer using nitrogen gas supplied at a constant pressure of  $1.4 \times 10^5 \text{ N m}^{-2}$ . The pressure at the reactor inlet after the nebulizer was  $27 \text{ N m}^{-2}$  above atmospheric pressure. The volume mean diameter and geometric standard deviation of the droplets produced by the nebulizer are  $5.1 \mu\text{m}$  and  $2.0$ , respectively [13]. The nebulized solution droplets, suspended by nitrogen carrier gas, were then carried into the high temperature reactor furnace where droplets evolved into final product particles by solvent evaporation and precursor decomposition. The precursor solution was delivered with a rate of  $0.006 \text{ cm}^3 \text{s}^{-1}$  ( $20 \text{ mL h}^{-1}$ ), and the nitrogen carrier gas flow rate was  $83 \text{ cm}^3 \text{s}^{-1}$  ( $5 \text{ L min}^{-1}$ ). The reactor consisted of a quartz tube,  $2.54 \text{ cm}$  diameter and  $76.2 \text{ cm}$  length, heated by two horizontal furnaces in series (both Lindberg, type 55035). The furnace set point temperature for experiments was chosen as  $1,000^\circ\text{C}$  to produce pure copper particles, as described elsewhere [14]. A differential mobility analyzer (TSI, Inc., Model 3071) was used to select certain particle sizes from the polydisperse aerosol by using a bipolar charger.

### 2. Size Classification by Electrical Mobility

Electrostatic classification of aerosols is the process by which aerosol particles are separated into classes according to their electric mobility. Electrostatic classification is accomplished with a differential mobility analyzer (DMA), consisting of an inner cylinder rod connected to a variable DC power supply and an outer annular tube connected to ground. Clean sheath air flows through the axial region while the charged aerosol enters through an axisymmetric opening along the outer cylinder. A schematic of a DMA is shown in Fig. 2. The charged aerosol particles move radially towards the center rod under the influence of the electric field. Near the bottom of the classifying region, a fraction of the airflow consisting of near-monodisperse aerosol is extracted through a slit in the center rod. The particles then flow to a condensation nucleus particle counter or an electrostatic precipitator. A typical measurement sequence is to measure the number concentration as a function of the applied

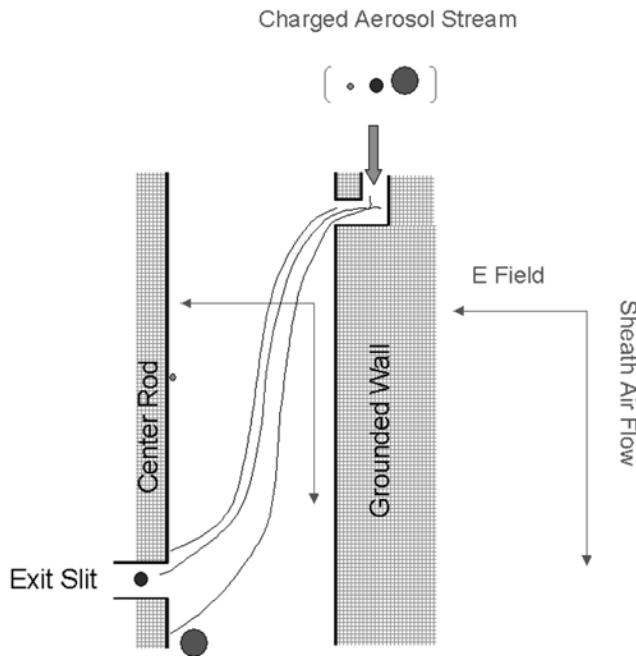


**Fig. 2. Schematic representation of particle paths under the influence of electric field in a differential mobility analyzer (DMA).**

voltage (particle size).

The quantity measured by the DMA is the electrical mobility,  $Z_p$ , defined as the velocity a particle attains under a unit electric field. Knutson and Whitby [12] derived an expression for the average value of  $Z_p$  for the particles entering the slit, involving the electrode voltage,  $V$ , the sheath air flow rate,  $Q_c$ , the inner and outer radii of the cylinders,  $r_1$  and  $r_2$ , and the length of the central electrode down to the slit,  $L$ .

$$Z_p = \frac{Q_c}{2\pi VL} \ln(r_2/r_1). \quad (15)$$

This equation is valid provided the sheath air flow,  $Q_c$ , is equal to the excess flow,  $Q_m$ , leaving the classifier. Knutson and Whitby [12] obtained the following expression for the range in the electrical mobility,  $\Delta Z_p$ , involving the inlet aerosol flow,  $Q_a$ .

$$\Delta Z_p = \frac{Q_a}{2\pi VL} \ln(r_2/r_1). \quad (16)$$

This equation is also valid provided the aerosol inlet flow,  $Q_a$ , is equal to the sampling flow,  $Q_s$ , leaving the aerosol outlet. The resolution limit of the size classification is given by the ratio of  $\Delta Z_p/Z_p$ .

$$\frac{\Delta Z_p}{Z_p} = \frac{Q_a}{Q_c}. \quad (17)$$

The electrical mobility,  $Z_p$ , of a singly charged particle can be derived by equating the electric field force,  $F_e$ , with the Stokes drag force,  $F_d$ :

$$\text{Stokes Drag Force: } F_d = \frac{3\pi\mu V D_p}{C(D_p)} \quad (18)$$

$$\text{Electric Field Force: } F_e = eE \quad (19)$$

$$\text{Electrical Mobility: } Z_p = \frac{V}{E} = \frac{eC(D_p)}{3\pi\mu D_p}, \quad (20)$$

Where

$V$  = radial component of particle velocity  
 $E$  = electric field strength  
 $e$  = elementary unit of charge  
 $C(D_p)$  = slip correction factor  
 $\mu$  = air viscosity  
 $D_p$  = particle diameter

The slip correction factor is given by [15],

$$C(D_p) = 1 + \left( \frac{2 \cdot \lambda}{D_p} \right) \cdot \left[ 1.165 + 0.483 \cdot \exp \left( -\frac{0.997 \cdot D_p}{2 \cdot \lambda} \right) \right], \quad [15] \quad (21)$$

which is valid from the free molecular to the continuum regimes, where  $\lambda$  is gas mean free path given;  $\lambda_0$  is 67.3 nm;  $\mu_0$  is  $1.8324 \times 10^{-5}$  Pa·s for air at  $T_0$ ,  $P_0$ .  $T_0$  is reference temperature, 296.15 K;  $P_0$  is reference pressure,  $1.0133 \times 10^5$  Pa (760 mmHg).

As seen from Eq. (20) and shown in Fig. 2, small particles have high electrical mobility, and thus move with high radial velocities toward the center rod and deposit on its surface. Larger particles, with lower electric mobility, are swept further down the classifying region before depositing on the center rod. Still larger particles are swept out the bottom of the classifier with the excess air. The monodisperse output of the classifier is extracted through a small slit on the center rod. Only particles with electric mobility within a narrow range have trajectories that bring them to the entrance of the slit. In this way, the classifier extracts a narrow size range of particles from the broader size range of particles entering the classifying region.

### 3. Particle Deposition

Size-classified 100 nm copper particles were passed through electric field, and the particles were deposited onto the selected area associated with experimental conditions such as aerosol flow rate, applied voltage, and separation distance between the aerosol inlet tube which is grounded and the substrate connected to high voltage power supply. Aerosol flow rate of  $100 \text{ cm}^3/\text{min}$  and 1 cm separation distance were used for depositions. Silicon wafers of one inch diameter were used as substrates for particle deposition, and those were further used for the light scattering measurements. Deposition area was checked with the cross scanning of the wafers, and the measured light intensity scattered from the particles was monitored as a function of the scanning distance.

### 4. Scattering Measurement

Samples of size-monodisperse 100 nm copper spheres were produced. Linearly polarized light of wavelength  $\lambda$  was incident upon each sample at an angle  $\theta$ . Light scattered into a direction defined by polar angle  $\theta$ , and azimuthal angle  $\phi$ , was detected, yielding a differential scattering cross section (DSC), and analyzed for polarization state. The DSC is given by

$$\frac{d\sigma}{d\Omega} = \frac{d\Phi_s \cos \theta}{d\Omega} \frac{\Phi_i}{\Phi_s}, \quad (22)$$

where  $\Phi_i$  and  $\Phi_s$  are the power of incident and scattered light, respectively, and  $d\Omega$  is the collection solid angle. The DSC relates the intensity at a single particle to the power scattered by it per solid angle. A goniometric optical scatter instrument, described elsewhere [16]

was used to perform the measurements. The laser beam ( $\lambda=532$  nm, Nd : YAG) at the sample was approximately 1 mm in diameter. The intensity was measured at  $\theta=35^\circ$  for  $\theta=30^\circ$  with  $\lambda=532$  nm.

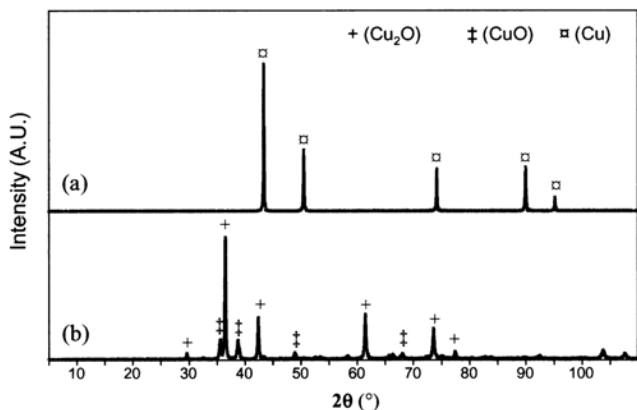


**Fig. 3. X-ray diffraction (XRD) patterns of copper particles prepared at 600 °C from 0.30 mol L<sup>-1</sup> copper nitrate in a) 10% volume fraction of ethanol in water and b) pure aqueous solutions, adapted from the reference [17].**

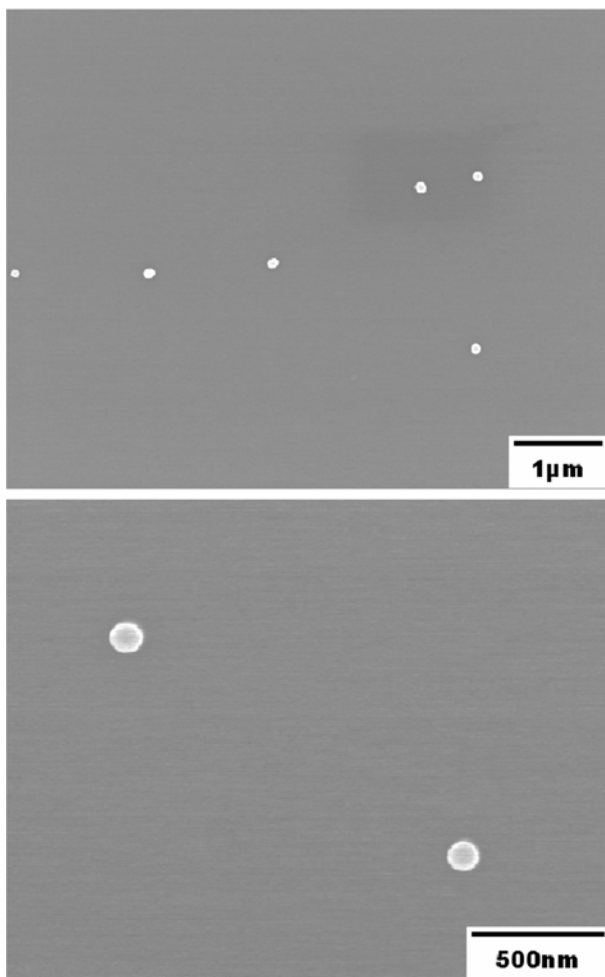


**Fig. 4. SEM images of copper nanoparticles produced at 1,000 °C from 0.3 mol/L copper nitrate precursor solution containing 10 volume% of ethanol.**

## RESULTS AND DISCUSSION

Particles generated at 1,000 °C by the spray pyrolysis were phase pure copper crystal. Fig. 3 shows X-ray diffraction patterns of copper particles prepared at 600 °C from 0.3 mol/L copper nitrate in 10 volume% of ethanol in water and pure aqueous solutions. These results [14,17] are adapted here to demonstrate the effect of ethanol cosolvent in production of pure copper particles from nitrate precursor. As shown, phase pure copper particles were obtained from the nitrate precursor with 10 volume% of ethanol at 600 °C, compared with the mixed crystals of pure copper and copper oxides. Phase pure copper particles were generated by using the nitrate precursor by incorporating with the ethanol cosolvent at temperatures above 600 °C. Phase purity is extremely important to apply materials for optical scattering measurements because the refractive index is strongly dependent on the material compositions. Therefore, the use of copper particles produced at 1,000 °C is safe for light scattering experiments.

The pure copper particles were size-classified through the DMA for 100 nm diameter. Fig. 4 shows the scanning electron microscopy images of 100 nm pure copper particles. Uniform size distribution can be seen in those two images. In order to obtain more statistical data for particle sizes, the geometric standard deviation (GSD) of

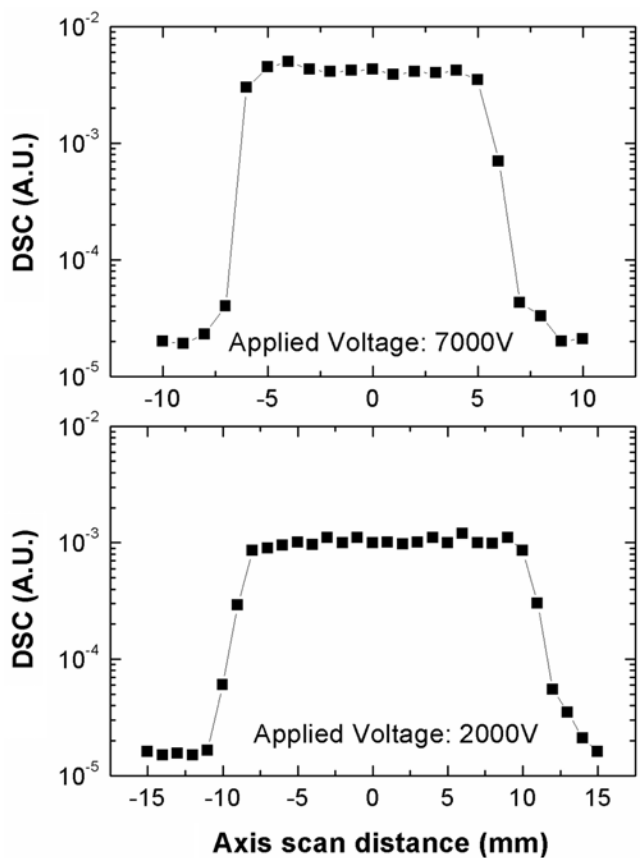


**Fig. 5. Results of deposition spot area scanned by the light scattering system for two different applied voltages. The separation distance between ground and high voltage rod is 1 cm. The spot diameters are about 1.4 cm by 7,000 V and 2.3 cm by 2,000 V. The intensity was measured at  $\theta=35^\circ$  for  $\theta=30^\circ$  with  $\lambda=532$  nm.**

**Table 1. Examples of the particle deposition area under various flow conditions. Aerosol flow rate and the separation distance were set as 100 cm<sup>3</sup>/sec and 1 cm, respectively**

Variables	D <sub>p</sub> (nm)	V (volt)	v <sub>E</sub> <sup>a</sup> (cm/s)	t <sub>p</sub> (sec)	r <sub>p</sub> /r <sub>0</sub>
Particle size	50	5000	2.36	0.765	1.22
	100	5000	0.67	2.19	1.79
	200	5000	0.22	4.69	3.47
	300	5000	0.12	6.40	5.45
Aerosol flow rate <sup>b</sup>	100	5000	0.67	1.79	2.58
Electric field	100	2000	0.27	4.10	2.96
	100	7000	0.94	1.69	1.56
Separation distance	100	5000	1.34 <sup>c</sup>	1.79	1.61
	100	5000	0.34 <sup>d</sup>	3.55	2.56

$$^a Z_p = v_E \cdot E, \text{ electrical mobility } Z_p = \frac{e \cdot C(D_p)}{3 \pi \mu D_p}.$$

<sup>b</sup>200 cm<sup>3</sup>/sec was used instead of 100 cm<sup>3</sup>/sec.

<sup>c</sup>1 cm of the separation distance.

<sup>d</sup>4 cm of the separation distance.

the particle sizes was calculated from about 50 transmission electron microscopy images [17] and it was 1.03.

Two deposition samples were prepared at two different applied voltages: 2,000 V and 7,000 V. Those samples were positioned at the center of the goniometric optical scatter instrument. The differential scattering cross section (DSC) was measured for both samples, and results are shown in Fig. 5. The x-axis in Fig. 5 is the distance crossing the diameter of the one inch wafer by scanning the DSC. The DSC is varied with the light intensity scattered by particles deposited, and the relative value shows the particle density change. Deposition distance at 7,000 V, the upper graph in Fig. 5, is about 1.4 cm, and it is very much similar to the particle deposition distance (1.56 cm) predicted in Table 1. In addition, the lower graph shows that the deposition distance is about 2.3 cm, and the predicted distance is 2.96 cm. Both examples show good agreement of the particle deposition area between the experimental measurements and the analytical predictions under the electric field conditions. Therefore, it is a good method to sample particulate matters on the specific area of the sampling substrates for off-line measurements.

An optical scatter instrument can also be used to measure particle number densities on silicon substrates if particle size and material property are clearly defined, and a few experimental results were reported [7,8]. In Fig. 5, there are little variations on the DSC values, but it is an almost negligible change compared to that of the background value. Those little fluctuations of the DSC values might come from the random distribution of particles in aerosol flow.

Several practical examples of deposition area for various flow conditions are shown in Table 1. As expected, the deposition area is increasing with increasing particle diameter because of the reduced particle mobility in large particles, and it is increased with increasing aerosol flow because of the increased inertial force of particles. For larger separation distance, the deposition area is increased because the precipitation time is increased and the particle velocity under the same electric field is reduced, so the deposition area is spread

more.

If there are large sized particles (>1 μm) for example, stronger particle deposition could happen at the center than the edge because of the multiple charges and because of the high electrical mobility from the high charges. However, controlled uniform particle deposition can be achieved with nanoparticles because nanoparticles mostly possess only one charge (+1 or -1).

## CONCLUSIONS

Pure copper nanoparticles were used for particle depositions under electric fields. Polydisperse copper particles were size-classified into uniform size through a DMA. Size-monodisperse particles can be obtained through a DMA by controlling the fluid flow rate and the electric field strength. Uniform size particles were then deposited on a silicon substrate to obtain a specific particle number density by controlling deposition parameters, and they can further be used for light scattering measurements. Light intensity (measured as differential scattering cross section, defined at Eq. (22)) scattered from the particles showed a relatively clear boundary for the deposition area. The experimental results were compared with the analytical estimations, and both results show good agreement. Therefore, electrophoresis can be used for particle sampling, especially for particles onto highly clean substrates without contamination issues and tight control of the deposition area.

## ACKNOWLEDGMENT

This work was supported by the research fund from the University of Seoul in 2006.

## NOMENCLATURE

r	: radial direction
z	: vertical direction
v <sub>1</sub>	: velocity component with respect to r direction [cm/s]
v <sub>2</sub>	: velocity component with respect to z direction [cm/s]
v <sub>3</sub>	: velocity component with respect to angle θ [cm/s]
Φ	: velocity potential
t	: time [s]
k	: arbitrary constant
t <sub>p</sub>	: precipitation time [s]
v <sub>E</sub>	: additional velocity component in the electric field direction [cm/s]
E	: electric field [V/cm]
Z <sub>p</sub>	: particle mobility under electric field [cm <sup>2</sup> /V·s]
Q <sub>c</sub>	: sheath air flow rate [cm <sup>3</sup> /s]
Q <sub>a</sub>	: inlet aerosol flow rate [cm <sup>3</sup> /s]
Q <sub>m</sub>	: excess flow rate leaving the classifier [cm <sup>3</sup> /s]
Q <sub>s</sub>	: sampling flow rate [cm <sup>3</sup> /s]
V	: center rod voltage [V], in Eq. (16)
L	: length of the central electrode [cm]
r <sub>1</sub>	: outer radius of center rod [cm]
r <sub>2</sub>	: inner radius of the outer cylinder [cm]
F <sub>e</sub>	: electric field force [g·cm/s <sup>2</sup> ]
F <sub>d</sub>	: Stokes drag force [g·cm/s <sup>2</sup> ]
V	: radial component of particle velocity [cm/s], in Eq. (20)

e	: elementary unit of charge [ $\text{g m}^2/\text{s}^2/\text{V}$ ]
C	: slip correction factor
$\mu$	: air viscosity [ $\text{g/m s}$ ]
$D_p$	: particle diameter [nm]
$\lambda$	: gas mean free path [nm]

## REFERENCES

1. K.-S. Kim, N. D. Demberelnyamba, S.-W. Yeon, S. Choi, J.-H. Chan and H. Lee, *Korean J. Chem. Eng.*, **22**, 717 (2005).
2. J.-W. Nah, Y.-I. Jeong and J.-J. Koh, *Korean J. Chem. Eng.*, **17**, 230 (2000).
3. J. Y. Park, S. G. Oh and B. H. Ha, *Korean J. Chem. Eng.*, **18**, 215 (2001).
4. D. J. Suh, O. O. Park, H.-T. Jung and M. H. Kwon, *Korean J. Chem. Eng.*, **19**, 529 (2002).
5. Y.-T. Yu and P. Mulvaney, *Korean J. Chem. Eng.*, **20**, 1176 (2003).
6. C. Y. Yun, S. Chah, S. K. Kang and J. Yi, *Korean J. Chem. Eng.*, **21**, 1062 (2004).
7. J. H. Kim, S. H. Ehrman, G. W. Mulholland and T. A. Germer, *Applied Optics*, **41**, 5405 (2002).
8. J. H. Kim, S. H. Ehrman, G. W. Mulholland and T. A. Germer, *Applied Optics*, **43**, 585 (2004).
9. K. Deppert, F. Schmidt, T. Krinke, J. Dixkens and H. Fissan, *J. Aerosol Science*, **27**, S151 (1996).
10. J. Dixkens and H. Fissan, *Aerosol Science and Technology*, **30**, 438 (1999).
11. J. C. Slattery, *Advanced transport phenomena*, Cambridge University, Cambridge (1999).
12. E. O. Knutson and K. T. Whitby, *J. Aerosol Science*, **6**, 443 (1975).
13. B. Y. H. Liu, *Fine particles: Aerosol generation, measurement, sampling, and analysis*, Academic Press, New York (1976).
14. J. H. Kim, V. I. Babushok, T. A. Germer, G. W. Mulholland and S. H. Ehrman, *J. Mater. Res.*, **18**, 1614 (2003).
15. J. H. Kim, G. W. Mulholland, S. C. Kukuck and D. Y. Pui, *J. Res. Natl. Inst. Stand. Technol.*, **110**, 31 (2005).
16. T. A. Germer and C. C. Asmail, *Rev. Sci. Instrum.*, **70**, 3688 (1999).
17. J. H. Kim, T. A. Germer, G. W. Mulholland and S. H. Ehrman, *Advanced Materials*, **14**, 518 (2002).